

## Supporting Information

### **Red-Emissive Carbon Quantum Dots Enable High Efficiency Luminescent Solar Concentrators**

Guiju Liu<sup>a,b,c,\*</sup>, Margherita Zavelani-Rossi<sup>d</sup>, Guangting Han<sup>a</sup>, Haiguang Zhao<sup>a,\*</sup>,  
Alberto Vomiero<sup>c,e,\*</sup>

<sup>a</sup> College of Textiles & Clothing, State Key Laboratory of Bio-Fibers and Eco-Textiles,  
Qingdao University, No. 308 Ningxia Road, Qingdao 266071, P.R. China. E-mail:  
hgzhao@qdu.edu.cn

<sup>b</sup> Department of Physics, Yantai University, Yantai 264005, P.R. China. E-mail:  
gjliu@ytu.edu.cn

<sup>c</sup> Division of Materials Science, Department of Engineering Sciences and Mathematics,  
Luleå University of Technology, 971 87 Luleå, Sweden. E-mail:  
alberto.vomiero@ltu.se

<sup>d</sup> Dipartimento di Energia, Politecnico di Milano, via G. Ponzio 34/3 and IFN-CNR,  
piazza L. da Vinci 32, 20133 Milano, Italy

<sup>e</sup> Department of Molecular Sciences and Nano Systems, Ca' Foscari University of  
Venice Via Torino 155, 30172 Venezia Mestre, Italy

## Supporting Figures

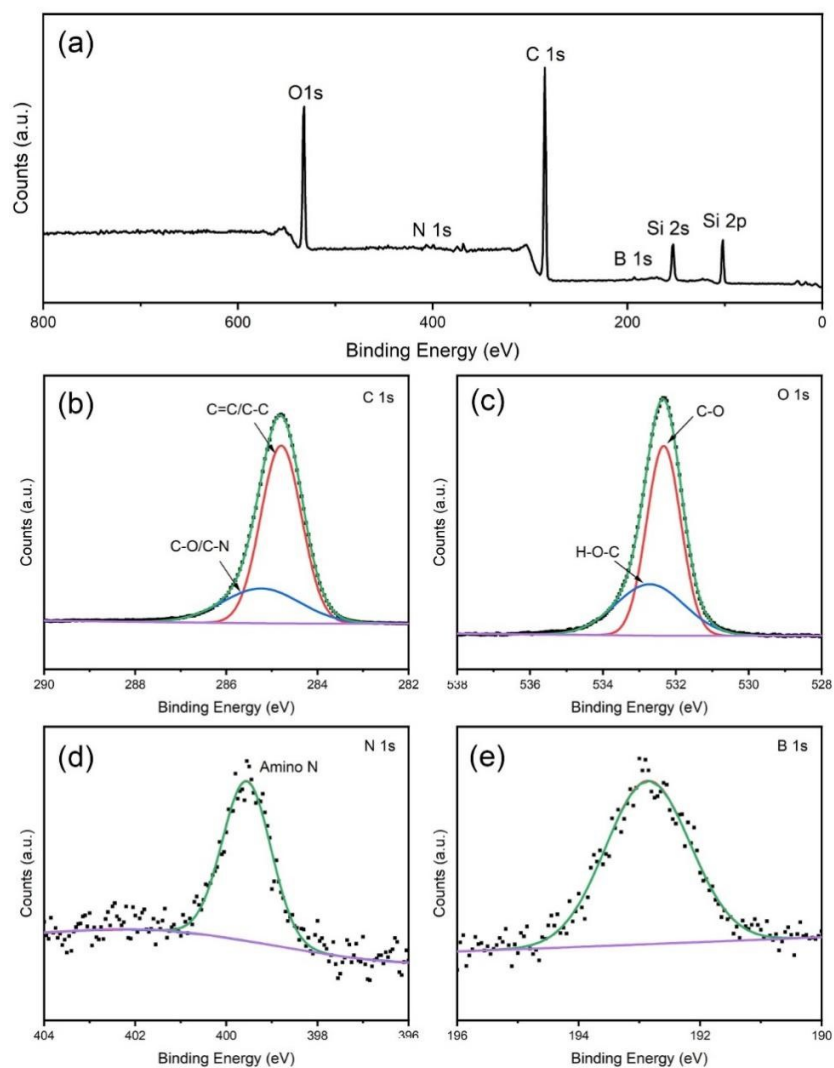


**Fig. S1** XPS full survey spectrum of the C-dots (a) and high resolution XPS spectra for C 1s (b), O 1s (c), N 1s (d) and B 1s (e).

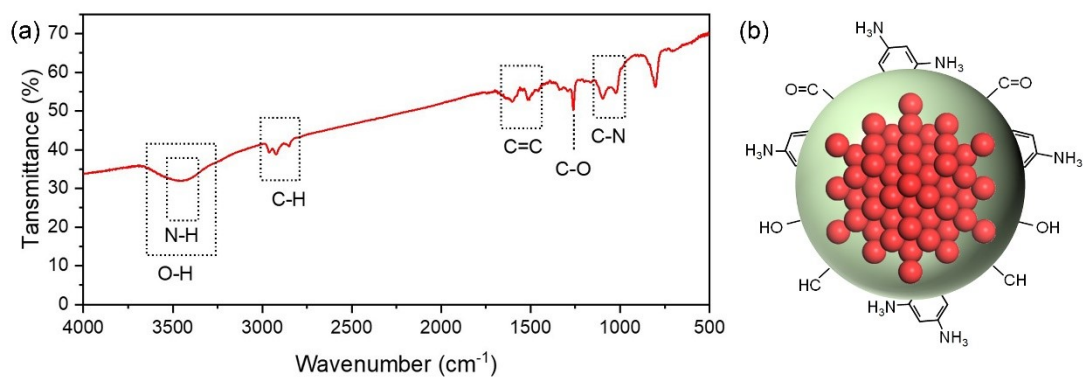


**Fig. S2** (a) FT-IR spectrum of the red-emissive C-dots. (b) Schematic diagram of the structure of C-dots.

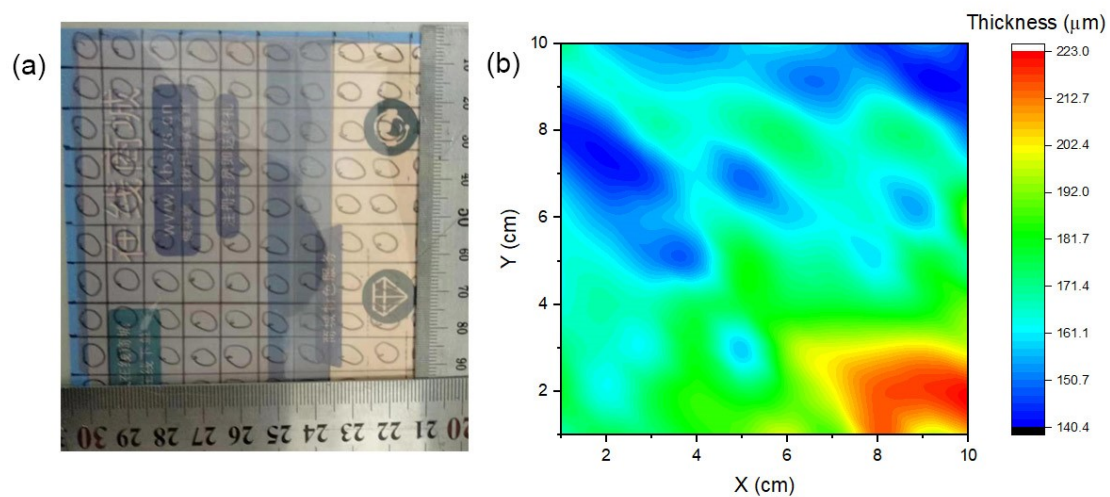


**Fig. S3** (a) photograph of the 10×10 cm<sup>2</sup> sized LSC based on C-dots/PMMA film. (b) 2D thickness distribution map of the LSC film.

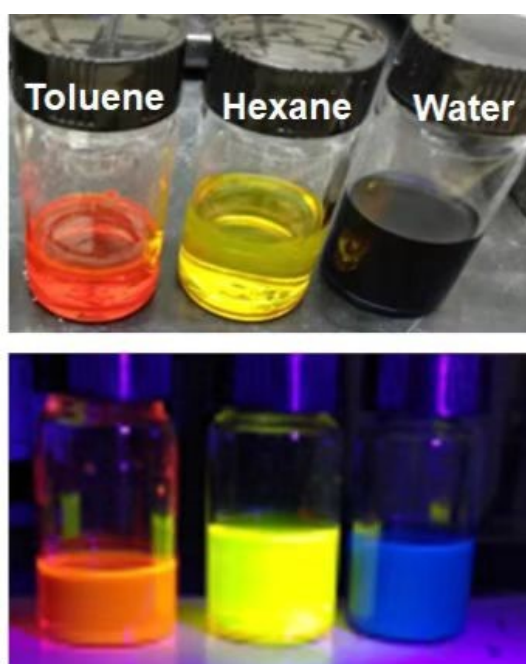


**Fig. S4** The photograph of the C-dots dispersed in different solution under indoor sunlight (top) and 365 nm UV light (bottom) irradiation.

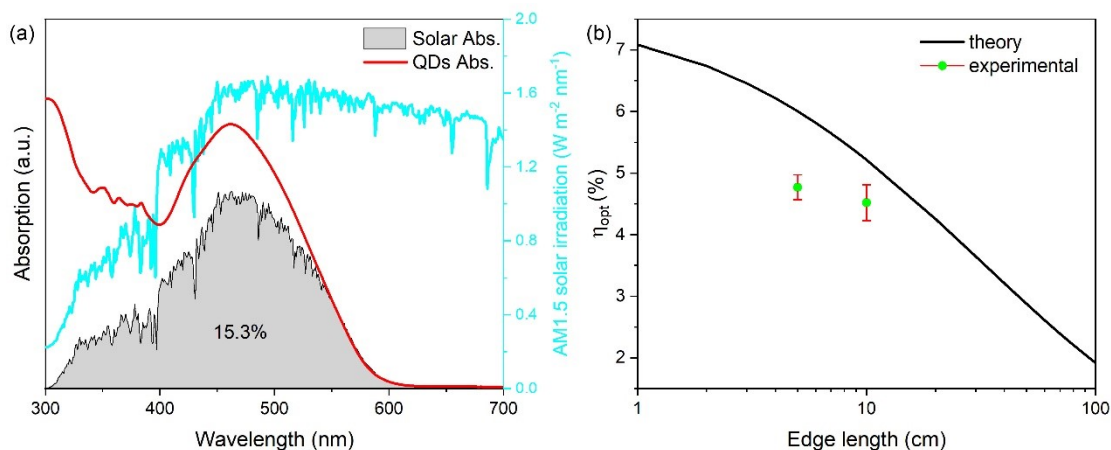


**Fig. S5** (a) Absorption spectrum of red-emissive C-dots used in LSC along with the AM 1.5 G solar spectrum. (b) Theoretical external optical efficiency ( $\eta_{\text{opt}}$ ) of the LSCs with different size under AM 1.5G sunlight illumination and the experimental  $\eta_{\text{opt}}$  of the LSCs ( $10 \times 10 \times 0.5 \text{ cm}^3$  and  $5 \times 5 \times 0.5 \text{ cm}^3$ ).

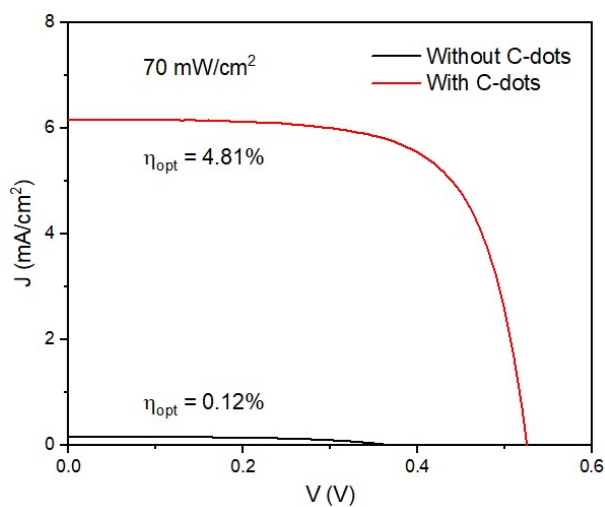


**Fig. S6** J-V curves of the LSC-solar cell with and without red-emissive C-dots under  $70 \text{ mW/cm}^2$  sunlight illumination. The LSC dimension is  $100 \text{ cm}^2$ .

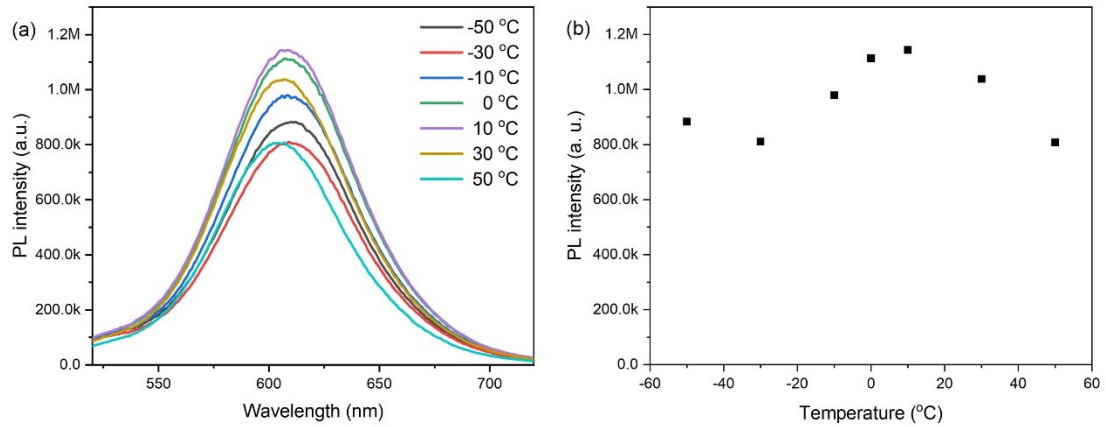


**Fig. S7** (a) Temperature dependent PL spectra for red-emissive C-dots based LSC. (b) The change of PL intensity under different temperature.

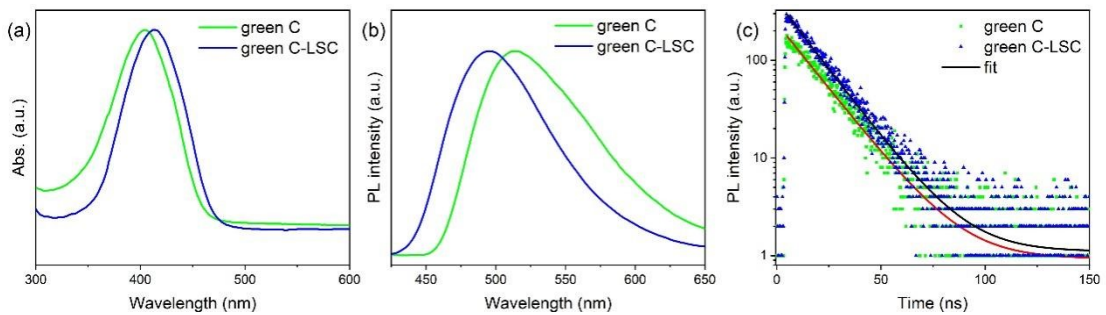


**Fig. S8** (a) Absorption, (b) PL emission spectra and (c) PL decay curves of the green-emissive C-dots in methanol and LSC.

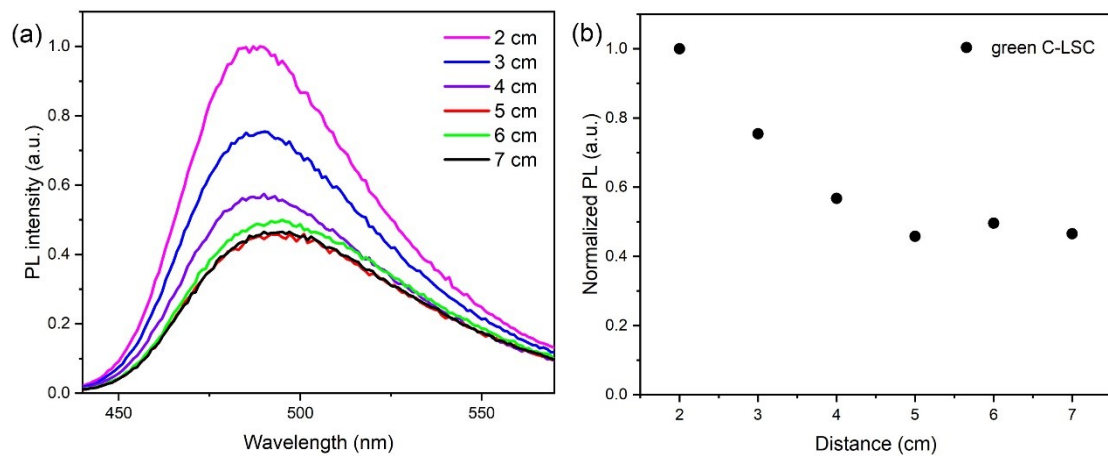


**Fig. S9** (a) PL spectra for different light propagation distance between the irradiation and the edge for green-emissive C-dots LSC. (b) Total PL intensity of the LSC as a function of distance of the irradiation from the side edge.

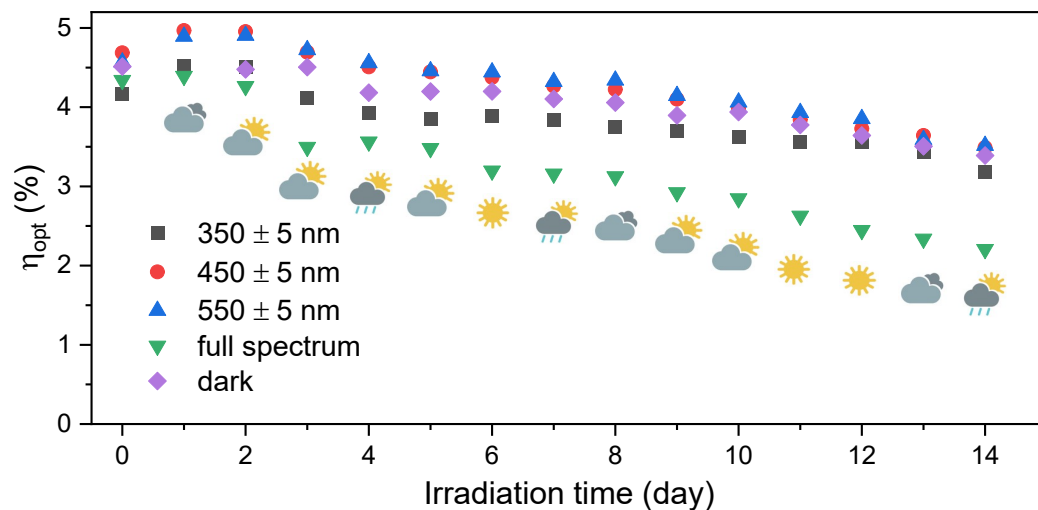


**Fig. S10** The longtime stability of the LSC under different wavelength of the sunlight irradiation ( $350 \pm 5$  nm,  $450 \pm 5$  nm,  $550 \pm 5$  nm, full solar spectrum and dark).

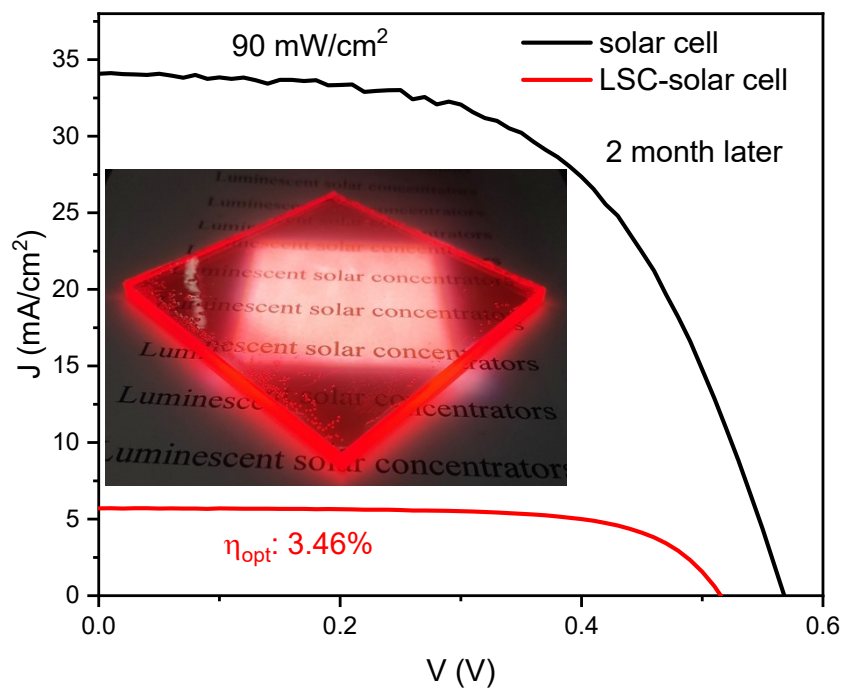


**Fig. S11** J-V curve of the red C-dots based LSC-solar cell placed in a nature room for 2 months.

Table S1. External optical efficiency for the LSCs based on C-dots.

Types of luminophore	Type of LSC	External optical efficiency (%)	LSC area (cm <sup>2</sup> )	Ref.
C-dots	Single	2.88	25	1
boric acid-graphene QDs	Single	2.5	100	2
C-dots	Single	2.7	100	3
	Single	2.2	225	
Ag40@SiO <sub>2</sub> /C-dots	Single	0.9	25	4
organosilane-functionalized C-dots	single	3.9	9	5
N-doped C-dots	single	4.52	12.5	6
C-dots	single	5.26	25	7
N-doped C-dots	single	5.02	3.24	8
N-doped C-dots	single	12.23	4	9
C-dots	laminated	1.6	100	10
N-doped C-dots	laminated	4.75	4	11
UV C-dots and visible C-dots	tandem	1.1	100	12
Red and yellow C-dots	tandem	4.3	100	13
Red, green and yellow C-dots	tandem	2.3	64	14
Red, green and yellow C-dots	tandem	4.03	6.25	15
C-dots				
CsPb(I <sub>x</sub> Br <sub>1-x</sub> ) <sub>3</sub>	tandem	3.05	100	16
CsPb(Cl <sub>x</sub> Br <sub>1-x</sub> ) <sub>3</sub>				
Red C-dots	single	4.81	100	This work
Green C-dots	single	3.0	100	This work
<b>Red C-dots and green C-dots</b>	<b>tandem</b>	<b>6.78</b>	<b>100</b>	<b>This work</b>

Table S2 Stability of LSCs based on various luminophores in previously reports.

Types of luminophore	$\eta_{\text{opt}}$ (%)	PCE (%)	Thermal stability	Long-term stability	Ref.
Cu-deficient	/	4.29	74% (40 °C)	/	17
CuGaAlS/ZnS core/shell QDs			50% (80 °C)		
Blue C-dots	2.61	/	287% (35 °C)	/	18
Green C-dots	2.76		261% (35 °C)		
Aggregation-induced emission molecules	4.2	1.4	/	70% (180 h)	19
C-dots	2.88	2.82	92% (70 °C)	~100% (14 days)	1
Cu <sub>4</sub> I <sub>6</sub> (pr-td) <sub>2</sub>	3.6	3.59	64% (70 °C)	~100% (14 days)	
Si-C-dots	7.58	6	/	83% (2 months)	20
CdSe/CdS QDs	2.3	/	80.4% (40 °C)	/	21
Red, yellow, green C-	4.03	2.92	/	89.3 (7 days)	15

dots					
Red C-dots	4.81	2.41	89% (60 °C)	72% (2 months)	This work

#### References:

1. Chen, J. C.; Zhao, H. G.; Li, Z. L.; Zhao, X. J.; Gong, X., Highly efficient tandem luminescent solar concentrators based on eco-friendly copper iodide based hybrid nanoparticles and carbon dots. *Energy & Environmental Science* 2022, 15 (2), 799-805.
2. Cai, K. B.; Huang, H. Y.; Hsieh, M. L.; Chen, P. W.; Chiang, S. E.; Chang, S. H.; Shen, J. L.; Liu, W. R.; Yuan, C. T., Two-Dimensional Self-Assembly of Boric Acid-Functionalized Graphene Quantum Dots: Tunable and Superior Optical Properties for Efficient Eco-Friendly Luminescent Solar Concentrators. *ACS Nano* 2022, 16 (3), 3994-4003.
3. Zhao, H.; Liu, G.; You, S.; Camargo, F. V. A.; Zavelani-Rossi, M.; Wang, X.; Sun, C.; Liu, B.; Zhang, Y.; Han, G.; Vomiero, A.; Gong, X., Gram-scale synthesis of carbon quantum dots with a large Stokes shift for the fabrication of eco-friendly and high-efficiency luminescent solar concentrators. *Energy & Environmental Science* 2021, 14 (1), 396-406.
4. Liu, X.; Benetti, D.; Rosei, F., Semi-transparent luminescent solar concentrators based on plasmon-enhanced carbon dots. *Journal of Materials Chemistry A* 2021, 9 (41), 23345-23352.
5. Talite, M. J.; Huang, H. Y.; Cai, K. B.; Capinig Co, K. C.; Cynthia Santoso, P. A.; Chang, S. H.; Chou, W. C.; Yuan, C. T., Visible-Transparent Luminescent Solar Concentrators Based on Carbon Nanodots in the Siloxane Matrix with Ultrahigh Quantum Yields and Optical Transparency at High-Loading Contents. *J Phys Chem Lett* 2020, 11 (2), 567-573.
6. Mateen, F.; Ali, M.; Oh, H.; Hong, S.-K., Nitrogen-doped carbon quantum dot based luminescent solar concentrator coupled with polymer dispersed liquid crystal device for smart management of solar spectrum. *Solar Energy* 2019, 178, 48-55.
7. Mateen, F.; Ali, M.; Lee, S. Y.; Jeong, S. H.; Ko, M. J.; Hong, S.-K., Tandem structured luminescent solar concentrator based on inorganic carbon quantum dots and organic dyes. *Solar Energy* 2019, 190, 488-494.
8. Wang, Z.; Zhao, X.; Guo, Z.; Miao, P.; Gong, X., Carbon dots based nanocomposite thin film for highly efficient luminescent solar concentrators. *Organic Electronics* 2018, 62, 284-289.
9. Gong, X.; Ma, W.; Li, Y.; Zhong, L.; Li, W.; Zhao, X., Fabrication of high-performance luminescent solar concentrators using N-doped carbon dots/PMMA mixed matrix slab. *Organic Electronics* 2018, 63, 237-243.
10. Zhao, H.; Liu, G.; Han, G., High-performance laminated luminescent solar concentrators based on colloidal carbon quantum dots. *Nanoscale Adv* 2019, 1 (12), 4888-4894.
11. Li, Y.; Miao, P.; Zhou, W.; Gong, X.; Zhao, X., N-doped carbon-dots for luminescent solar concentrators. *J. Mater. Chem. A* 2017, 5 (40), 21452-21459.



12. Zhou, Y.; Benetti, D.; Tong, X.; Jin, L.; Wang, Z. M.; Ma, D.; Zhao, H.; Rosei, F., Colloidal carbon dots based highly stable luminescent solar concentrators. *Nano Energy* 2018, 44, 378-387.
13. Li, J. R.; Zhao, H. G.; Zhao, X. J.; Gong, X., Red and yellow emissive carbon dots integrated tandem luminescent solar concentrators with significantly improved efficiency. *Nanoscale* 2021, 13 (21), 9561-9569.
14. Zdrazil, L.; Kalytchuk, S.; Hola, K.; Petr, M.; Zmeskal, O.; Kment, S.; Rogach, A. L.; Zboril, R., A carbon dot-based tandem luminescent solar concentrator. *Nanoscale* 2020, 12 (12), 6664-6672.
15. Wang, J.; Wang, J.; Xu, Y.; Jin, J.; Xiao, W.; Tan, D.; Li, J.; Mei, T.; Xue, L.; Wang, X., Controlled Synthesis of Long-Wavelength Multicolor-Emitting Carbon Dots for Highly Efficient Tandem Luminescent Solar Concentrators. *ACS Applied Energy Materials* 2020, 3 (12), 12230-12237.
16. Zhao, H.; Benetti, D.; Tong, X.; Zhang, H.; Zhou, Y.; Liu, G.; Ma, D.; Sun, S.; Wang, Z. M.; Wang, Y.; Rosei, F. Efficient and Stable Tandem Luminescent Solar Concentrators Based on Carbon dots and Perovskite Quantum dots. *Nano Energy* 2018, 50, 756-765.
17. You, Y.; Tong, X.; Imran Channa, A.; Zhi, H.; Cai, M.; Zhao, H.; Xia, L.; Liu, G.; Zhao, H.; Wang, Z., High-efficiency luminescent solar concentrators based on Composition-tunable Eco-friendly Core/shell quantum dots. *Chemical Engineering Journal* 2023, 452, 139490.
18. Xu, B.; Wang, J.; Cai, C.; Xin, W.; Wei, L.; Yang, Q.; Peng, B.; Hu, Y.; Li, J.; Wang, X., Construction of Laminated Luminescent Solar Concentrator "Smart" Window Based on Thermoresponsive Polymer and Carbon Quantum Dots. *Crystals* 2022, 12,1612.
19. Li, X.; Qi, J.; Zhu, J.; Jia, Y.; Liu, Y.; Li, Y.; Liu, H.; Li, G.; Wu, K., Low-Loss, High-Transparency Luminescent Solar Concentrators with a Bioinspired Self-Cleaning Surface. *J Phys Chem Lett* 2022, 13 (39), 9177-9185.
20. Wu, J.; Xin, W.; Wu, Y.; Zhan, Y.; Li, J.; Wang, J.; Huang, S.; Wang, X., Solid-state photoluminescent silicone-carbon dots/dendrimer composites for highly efficient luminescent solar concentrators. *Chemical Engineering Journal* 2021, 422, 130158.
21. Liu, B. X.; Ren, S. H.; Han, G. T.; Zhao, H. G.; Huang, X. Y.; Sun, B.; Zhang, Y. M., Thermal effect on the efficiency and stability of luminescent solar concentrators based on colloidal quantum dots. *Journal of Materials Chemistry C* 2021, 9 (17), 5723-5731.